J. Comput. Appl. Res. Mech. Eng. Vol. 11. No. 2, pp. 317-327, 2022 DOI: 10.22061/JCARME.2021.4994.1607

Journal of Computational and Applied Research in Mechanical Engineering

jcarme.sru.ac.ir

SRTTU

JCARME

ISSN: 2228-7922

Research paper

Role of ohmic heating and radiation on magnetohydrodynamic Jeffery fluid model through a tapered channel with peristalsis

S. Ravikumar*, D. Vijaya Sekhar and Sk. Abzal

Department of Mathematics, NBKR Institute of Science and Technology (An Autonomous Institution, Accredited by NBA and 'A'- Grade of NAAC, ISO 9001:2008 Certified), Vidyanagar, SPSR Nellore, Andhra Pradesh-524413, India

Article info:

Article history:

Received: 16/03/2019

Revised: 25/08/2021

Accepted: 30/08/2021

Online: 04/09/2021

Keywords:

Ohmic heating,

Radiation,

Gravity field,

MHD,

Tapered channel.

***Corresponding author:**

drsravikumar1979@gmail.com

Abstract

Theoretical investigation of Ohmic heating (Joule heating) and radiation on MHD Jeffery fluid model with porous material along the tapered channel with peristalsis is the focus of this study. Long wavelength and low-Reynolds number approximations are used in the mathematical modelling. Axial rate, pressure gradient, temperature, and heat transfer coefficient rate expressions are calculated. Plotting diagrams were used to analyse the impact of physical parameters on flow characteristics, which were then addressed in greater depth. It is worth noting that raising the gravitational parameter, Jeffery fluid parameter, Hartmann number and Porosity parameter raises the fluid's velocity. Also, as the Ohmic heating (Jeffery fluid) parameter and porosity parameter increase, the axial pressure gradient drop;, and the temperature of the fluid rises. The rate of heat transfer coefficient rises in region $x \in [0.55,1]$ with an increase in the Radiation parameter, Heat generator parameter and Jeffery fluid parameter. Mathematica software is employed to seek out numerical results.

1. Introduction

To the best of our knowledge, no investigation has been made yet to examine an impression of Ohmic heating (Joule heating) and radiation on MHD Jeffery fluid model in a vertical asymmetric tapering channel with peristalsis. The investigation of the mechanisms of peristalsis, in each physiological and mechanical situation, has been scientifically examined quite slowly. The fundamental principles of peristaltic pumping were demonstrated in two – dimensional channel and highlighting the impact of various factors on regulating flow as outlined by Jaffrin and Shapiro [1], Fung and Yih [2] and Shapiro et al. [3]. A numerical model for peristaltic motion of a Newtonian fluid was designed by Kothandapani and Prakash [4]. Bhatti et al. [5] discussed the mathematical modelling of heat and mass transfer consequences on MHD peristaltic flow. Free convection flow by elicited force field has been

mentioned by Ghosh et al. [6]. The in-depth literature on the present analysis can be found in the following references: Ameer Ahamad et al.[7] Makinde et al. [8], Sinha et al. [9], Akram and Nadeem [10], Ellahi [11], Rashidi et al.[12], Gnaneswara Reddy and Makinde [13], Bhatti et al. [14], Hayat et al. [15], Gnaneswara Reddy et al. [16], Veeresh et al. [17], Vajravelu et al. [18], Eldabe et al. [19], Asha and Sunitha [20], Nehad Ali Sha et al. [21] and several other therein. Recently, Chamkha et al. [22] designed the MHD flow and heat transfer of a hybrid nanofluid in a rotating system.

The primary goal of the current study is to examine the impact of Ohmic heating and radiation on the MHD Jeffery fluid model in a channel with peristalsis; it has escaped the consideration of earlier scholars. Up to now numerous researchers have examined peristaltic Jeffery fluid model with heat transfer through various channels like symmetric channel, planner channel, asymmetric channel, asymmetric vertical channel, tapered channel and also circular cylindrical tube, inclined circular tube and finite length tube with permeable walls.

As previously stated, the current research has a broad range of applications in the polymer industry, as well as biomedical engineering, clinical diagnosis, and surgery, all of which involve flows through porous media in the presence of a magnetic field and radiation. The model established has been employed to explore the dynamics of blood flow in ill arteries under the influence of an external magnetic field, when the artery lumen transforms into a porous structure and blood functions like a plastic fluid.

2. Formulation of the problem

On the MHD Jeffery fluid model, we consider an incompressible viscous fluid flow with Ohmic heating through a channel with peristalsis. The porous medium and radiation are also taken into account.

The wall surface of the problem is labeled by (Fig. 1):

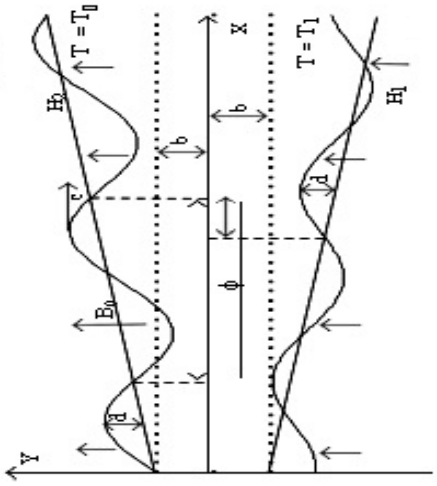

Fig. 1. Schematic diagram of the physical mode.

$$Y = \overline{H_2} = b + m^I \bar{X} + d \sin\left[\frac{2\pi}{\lambda}\left(\bar{X} - c\bar{t}\right)\right] \quad (1)$$

$$Y = \overline{H_2} = b + m^I \bar{X} + d \sin\left[\frac{2\pi}{\lambda}\left(\bar{X} - c\bar{t}\right)\right] \quad (2)$$

where b, d, c, m', t, λ *and* ϕ are mean half-width of the channel, amplitude of the peristaltic wave, phase speed, non-uniform parameter, time, wavelength and phase difference.

Constitutive equations of the Jeffrey fluid are as follows:

$$\bar{T} = -\bar{p}\bar{I} + \bar{S} \quad (3)$$

$$\bar{S} = \frac{\mu}{1 + \lambda_1\left(\bar{\dot{r}} + \lambda_2 \bar{\ddot{r}}\right)} \quad (4)$$

The governing equations of the current study are as follows [23]:

$$\frac{\partial \bar{u}}{\partial \bar{x}} + \frac{\partial \bar{v}}{\partial \bar{y}} = 0 \quad (5)$$

$$\rho\left(\bar{u}\frac{\partial \bar{u}}{\partial \bar{x}} + \bar{v}\frac{\partial \bar{u}}{\partial \bar{y}}\right) = -\frac{\partial p}{\partial x} + \frac{\partial \bar{S}_{\bar{xx}}}{\partial \bar{x}} + \frac{\partial \bar{S}_{\bar{xy}}}{\partial \bar{y}}$$

$$-\sigma B_0^{\,2}\bar{u} - \frac{\mu}{k_1}\bar{u} + \rho g \sin\alpha \quad (6)$$

$$\rho\left(\bar{u}\frac{\partial \bar{v}}{\partial \bar{x}} + \bar{v}\frac{\partial \bar{v}}{\partial \bar{y}}\right) = -\frac{\partial p}{\partial \bar{y}} + \frac{\partial \bar{S}_{\bar{xy}}}{\partial \bar{x}} + \frac{\partial \bar{S}_{\bar{yy}}}{\partial \bar{y}}$$

$$-\sigma B_0^{\,2}\bar{v}-\frac{\mu}{k_1}\bar{v}+\rho g\cos\alpha \tag{7}$$

$$\rho C_p\left(\bar{u}\frac{\partial}{\partial\bar{x}}+\bar{v}\frac{\partial}{\partial\bar{y}}\right)\bar{T}=k\left(\frac{\partial^2}{\partial\bar{x}^2}+\frac{\partial^2}{\partial\bar{y}^2}\right)\bar{T}$$
$$+Q_0+\sigma B_0^{\,2}\bar{u}^2-\frac{\partial q}{\partial\bar{y}} \tag{8}$$

where

$$\bar{S}_{\bar{xx}}=\frac{2\mu}{1+\lambda_1}\left(1+\lambda_2\left(\bar{u}\frac{\partial}{\partial\bar{x}}+\bar{v}\frac{\partial}{\partial\bar{y}}\right)\right)\frac{\partial\bar{u}}{\partial\bar{x}},$$

$$\bar{S}_{\bar{xy}}=\frac{\mu}{1+\lambda_1}\left(1+\lambda_2\left(\bar{u}\frac{\partial}{\partial\bar{x}}+\bar{v}\frac{\partial}{\partial\bar{y}}\right)\right)\left(\frac{\partial\bar{u}}{\partial\bar{y}}+\frac{\partial\bar{v}}{\partial\bar{x}}\right),$$

$$\bar{S}_{\bar{yy}}=\frac{2\mu}{1+\lambda_1}\left(1+\lambda_2\left(\bar{u}\frac{\partial}{\partial\bar{x}}+\bar{v}\frac{\partial}{\partial\bar{y}}\right)\right)\frac{\partial\bar{u}}{\partial\bar{y}}.$$

where $\bar{u}and\bar{v}\ k_1\ \rho\ k\ \mu\ Q_0\ C_p\ and\bar{T}$ are velocity components, permeability of the porous medium, density of the fluid, thermal conduction, coefficient of the viscosity, constant heat addition, specific heat at constant pressure, and temperature of the fluid.

The radioactive heat flux (Cogley et al. [24]) is given by $\frac{\partial q}{\partial y}=4\alpha^2\left(T_0-T_1\right)$, here α is the mean radiation absorption coefficient.

Introducing the following non-dimensional quantities:

$$\left.\begin{aligned}
&x=\frac{\bar{x}}{\lambda},y=\frac{\bar{y}}{b},\bar{t}=\frac{ct}{\lambda},u=\frac{\bar{u}}{c},v=\frac{\bar{v}}{c\delta},\\
&S=\frac{b\bar{S}}{\mu c},h_1=\frac{\overline{H_1}}{b},h_2=\frac{\overline{H_2}}{b},p=\frac{b^2\bar{p}}{c\lambda\mu},\\
&\theta=\frac{\bar{T}-T_0}{T_1-T_0},\delta=\frac{b}{\lambda},Re=\frac{\rho cb}{\mu},M=B_0b\sqrt{\frac{\sigma}{\mu}},\\
&P_r=\frac{\mu C_p}{k},E_c=\frac{c^2}{C_p\left(T_1-T_0\right)},\varepsilon=\frac{d}{b},\eta=\frac{\rho b^2g}{\mu c},\\
&\eta_1=\frac{\rho b^3g}{\lambda\mu c},\ \beta=\frac{Q_0b^2}{\mu C_p\left(T_1-T_0\right)},N^2=\frac{4\alpha^2d^2}{k}.
\end{aligned}\right\} \tag{9}$$

where $Re\ M\ Pr\ E\,c\ \beta\ \eta and\eta_1\ N\ and\ Br$ are Reynolds number, Hartmann number, Prandtl number, Eckert number, heat sink parameter, gravitational parameters, Radiation parameter and Brinkman number.

3. Solution of the problem

Substituting non-dimensional quantities (Eq. (9)) into Eqs. (5-8), we get the resultant equations after dropping the bars:

$$\delta\left(u\frac{\partial u}{\partial x}+v\frac{\partial v}{\partial y}\right) \tag{10}$$

$$Re\,\delta\left(u\frac{\partial u}{\partial x}+v\frac{\partial u}{\partial y}\right)=-\frac{\partial p}{\partial x}+\delta\frac{\partial S_{xx}}{\partial x}$$
$$+\frac{\partial S_{xy}}{\partial y}-M^2u-\frac{1}{Da}u+\eta\sin\alpha \tag{11}$$

$$Re\,\delta^3\left(u\frac{\partial v}{\partial x}+v\frac{\partial v}{\partial y}\right)=-\frac{\partial p}{\partial y}+\delta^2\frac{\partial S_{xy}}{\partial x}+\delta\frac{\partial S_{yy}}{\partial y}$$
$$-\delta^2M^2v-\delta^2\frac{1}{Da}u-\eta_1\cos\alpha \tag{12}$$

$$Re\,\delta\left(u\frac{\partial\theta}{\partial x}+v\frac{\partial\theta}{\partial y}\right)=\frac{1}{P_r}\left(\theta^2\frac{\partial^2\theta}{\partial x^2}+\frac{\partial^2\theta}{\partial y^2}\right)$$

$$+\beta+M^2Eu^2+\frac{N^2\theta}{P_r} \tag{13}$$

where

$$S_{xx}=\frac{2\delta}{1+\lambda_1}\left(1+\frac{\lambda_2\delta c}{d}\left(u\frac{\partial}{\partial x}+v\frac{\partial}{\partial y}\right)\right)\frac{\partial u}{\partial x},$$

$$S_{xy}=\frac{1}{1+\lambda_1}\left(1+\frac{\lambda_2\delta c}{d}\left(u\frac{\partial}{\partial x}+v\frac{\partial}{\partial y}\right)\right)\left(\frac{\partial u}{\partial x}+\delta^2\frac{\partial v}{\partial x}\right),$$

$$S_{yy}=\frac{2}{1+\lambda_1}\left(1+\frac{\lambda_2\delta c}{d}\left(u\frac{\partial}{\partial x}+v\frac{\partial}{\partial y}\right)\right)\frac{\partial v}{\partial y}.$$

We use a long wavelength approximation, ignoring wave number (δ) and a low Reynolds number. Eqs. (10-13) become:

$$\frac{\partial^2u}{\partial y^2}-\left(M^2+\frac{1}{Da}\right)\left(1+\lambda_1\right)u=\left(1+\lambda_1\right)\frac{\partial p}{\partial x}$$

$$-\eta \sin\alpha\left(1+\lambda_1\right) \tag{14}$$

$$\frac{\partial p}{\partial y}+\eta_1 \cos\alpha = 0 \tag{15}$$

$$\frac{\partial^2\theta}{\partial y^2}+N^2\theta = -\beta P_r - M^2 B_r u^2 \tag{16}$$

The dimensionless boundary conditions are:

$$u=-1,\ \theta=0 \ at\ \ y=h_1 \tag{17}$$

$$u=-1, \theta=1 \ at\ \ y=h_2 \tag{18}$$

where

$$h_1 = -1-k_1 x-\varepsilon\ \sin\left[2\pi\left(x-t\right)+\phi\right],$$

$$h_2 = 1+k_1 x+\varepsilon\ \sin\left[2\pi\left(x-t\right)\right].$$

Solving the Eqs. (14)-(16) by using the boundary conditions (17) and(18), we get:

$$u = b_1 \sinh\left[\alpha_1 y\right]+b_2 \cosh\left[\alpha_1 y\right]+A \tag{19}$$

where

$$b_1 = \left(\frac{-1-A}{a_1}\right)a,\ \ b_2 = \left(\frac{-1-A}{a_1}\right),$$

$$a_1 = \left(\frac{\cosh\left[\alpha_1 h_2\right]-\cosh\left[\alpha_1 h_1\right]}{\sinh\left[\alpha_1 h_1\right]-\sinh\left[\alpha_1 h_2\right]}\right)\sinh\left[\alpha_1 h_1\right] + \cosh\left[\alpha_1 h_1\right],$$

$$a_2 = \left(\frac{\cosh\left[\alpha_1 h_2\right]-\cosh\left[\alpha_1 h_1\right]}{\sinh\left[\alpha_1 h_1\right]-\sinh\left[\alpha_1 h_2\right]}\right),$$

$$\alpha_1 = \sqrt{\left(1+\lambda_1\right)\left(M^2+\frac{1}{Da}\right)},$$

$$A = \left(\frac{-\frac{\partial p}{\partial x}+\eta\ \sin\alpha}{\left(M^2+\frac{1}{Da}\right)}\right).$$

$$\theta = b_9 \cos\left[N\,y\right]+b_8 \sin\left[Ny\right]-\left(\frac{\beta P_r}{N^2}\right) -\left(\frac{M^2 B_r b_3}{4\alpha_1^{\,2}+N^2}\right)\left(e^{2\alpha_1 y}\right)-\left(\frac{M^2 B_r b_4}{4\alpha_1^{\,2}+N^2}\right)\left(e^{-2\alpha_1 y}\right) -\left(\frac{M^2 B_r b_5}{\alpha_1^{\,2}+N^2}\right)\left(e^{\alpha_1 y}\right)-\left(\frac{M^2 B_r b_6}{\alpha_1^{\,2}+N^2}\right)\left(e^{-\alpha_1 y}\right) -\left(\frac{M^2 B_r b_7}{N^2}\right) \tag{20}$$

where

$$b_3 = \left(\frac{b_1^{\,2}}{4}+\frac{b_2^{\,2}}{4}+\frac{b_1 b_2}{2}\right),\ b_4 = \left(\frac{b_1^{\,2}}{4}+\frac{b_2^{\,2}}{4}-\frac{b_1 b_2}{2}\right),$$

$$b_5 = A\left(b_1+b_2\right),\ b_6 = A\left(b_1-b_2\right),$$

$$b_7 = \left(\frac{-b_1^{\,2}}{2}+\frac{b^2}{2}+A^2\right),$$

$$b_8 = b_{10}-b_{11}-b_{12}-b_{13}-b_{14}-b_{15}-b_{16},$$

$$b_9 = \left(\frac{-b_8 \sinh\left[Nh_1\right]+\left(\frac{\beta P_r}{N^2}\right)}{\cosh\left[Nh_1\right]}\right)+ \left(\frac{\left(\frac{M^2 B_r b_3}{4\alpha_1^{\,2}+N^2}\right)\left(e^{2\alpha_1 h_1}\right)+\left(\frac{M^2 B_r b_4}{4\alpha_1^{\,2}+N^2}\right)\left(e^{-2\alpha_1 h_1}\right)}{\cosh\left[Nh_1\right]}\right)+ \left(\frac{\left(\frac{M^2 B_r b_5}{\alpha_1^{\,2}+N^2}\right)\left(e^{\alpha_1 h_1}\right)+\left(\frac{M^2 B_r b_6}{\alpha_1^{\,2}+N^2}\right)\left(e^{-\alpha_1 h_1}\right)}{\cosh\left[Nh_1\right]}\right)+ \left(\frac{\left(\frac{M^2 B_r b_7}{N^2}\right)}{\cosh\left[Nh_1\right]}\right),\ b_{10} = \left(\frac{-\cosh\left[N\,h_1\right]}{F}\right),$$

$$b_{11}=\left(\frac{\left(\frac{\beta P_r}{N^2}\right)\left(\cosh\left[Nh_1\right]-\cosh\left[Nh_2\right]\right)}{F}\right),$$

$$b_{12}=\left(\frac{d_1\left(e^{2\alpha_1 h_2}\cosh\left[Nh_1\right]-e^{2\alpha_1 h_1}\cosh\left[Nh_2\right]\right)}{F}\right),$$

$$b_{13}=\left(\frac{d_2\left(e^{-2\alpha_1 h_2}\cosh\left[Nh_1\right]-e^{-2\alpha_1 h_1}\cosh\left[Nh_2\right]\right)}{F}\right),$$

$$b_{13}=\left(\frac{d_2\left(e^{-2\alpha_1 h_2}\cosh\left[Nh_1\right]-e^{-2\alpha_1 h_1}\cosh\left[Nh_2\right]\right)}{F}\right),$$

$$b_{14}=\left(\frac{d_3\left(e^{\alpha_1 h_2}\cosh\left[Nh_1\right]-e^{\alpha_1 h_1}\cosh\left[Nh_2\right]\right)}{F}\right),$$

$$b_{15}=\left(\frac{d_4\left(e^{-\alpha_1 h_2}\cosh\left[Nh_1\right]-e^{-\alpha_1 h_1}\cosh\left[Nh_2\right]\right)}{F}\right),$$

$$b_{16}=\left(\frac{d_5\left(\cosh\left[Nh_1\right]-\cosh\left[Nh_2\right]\right)}{F}\right),$$

$$F=\sinh\left[Nh_1\right]\cosh\left[Nh_2\right]-\sinh\left[\alpha_1 h_2\right]\cosh\left[Nh_1\right],$$

$$d_1=\left(\frac{M^2B_rb_3}{4\alpha_1^2+N^2}\right),\ d_2=\left(\frac{M^2B_rb_4}{4\alpha_1^2+N^2}\right),$$

$$d_3=\left(\frac{M^2B_rb_5}{\alpha_1^2+N^2}\right),\ d_4=\left(\frac{M^2B_rb_6}{\alpha_1^2+N^2}\right),$$

$$d_5=\left(\frac{M^2B_rb_6}{N^2}\right).$$

The heat transfer coefficient (Z) at $y=h_1\ and\ y=h_2$ walls, as calculated by:

$$Zh_1=\theta_y h_{1x} \tag{21}$$

$$Zh_2=\theta_y h_{2x} \tag{22}$$

The coefficient of heat transfer solutions at $y=h_1\ and\ y=h_2$ are:

$$Z=H\left(2\pi\grave{o}\ \cos\left[2\pi\left(x-t\right)+\phi\right]-k_1\right) \tag{23}$$

where

$$H=-b_9N\ \sin\left[Ny\right]+b_8N\cos\left[Ny\right]-2\alpha_1\left(\frac{M^2B_rb_3}{4\alpha_1^2+N^2}\right)\left(e^{2\alpha_1 y}\right)+2\alpha_1\left(\frac{M^2B_rb_4}{4\alpha_1^2+N^2}\right)\left(e^{-2\alpha_1 y}\right)-\alpha_1\left(\frac{M^2B_rb_5}{\alpha_1^2+N^2}\right)\left(e^{\alpha_1 y}\right)+\alpha_1\left(\frac{M^2B_rb_6}{\alpha_1^2+N^2}\right)\left(e^{-\alpha_1 y}\right)$$

$$Z=J\left(2\pi\grave{o}\ \cos\left[2\pi\left(x-t\right)\right]+k_1\right) \tag{24}$$

where

$$J=-b_9N\ \sin\left[Ny\right]+b_8N\cos\left[Ny\right]-2\alpha_1\left(\frac{M^2B_rb_3}{4\alpha_1^2+N^2}\right)\left(e^{2\alpha_1 y}\right)+2\alpha_1\left(\frac{M^2B_rb_4}{4\alpha_1^2+N^2}\right)\left(e^{-2\alpha_1 y}\right)-\alpha_1\left(\frac{M^2B_rb_5}{\alpha_1^2+N^2}\right)\left(e^{\alpha_1 y}\right)+\alpha_1\left(\frac{M^2B_rb_6}{\alpha_1^2+N^2}\right)\left(e^{-\alpha_1 y}\right)$$

In the wave frame, the volumetric flow rate is measured by:

$$q=\int_{h_1}^{h_2}u\,dy$$

$$=\int_{h_1}^{h_2}\left(a_1\,\mathrm{Sin}\,h\left[\alpha_1 y\right]+a_2\,\mathrm{Cos}\,h\left[\alpha_1 y\right]+A\right)dy$$

$$=\left(\frac{a_1}{\alpha_1}\right)\left(\mathrm{Cos}\,h\left[\alpha_1 h_2\right]-\mathrm{Cos}\,h\left[\alpha_1 h_1\right]\right)+\left(\frac{a_2}{\alpha_1}\right)\left(\mathrm{Sin}\,h\left[\alpha_1 h_2\right]-\mathrm{Sin}\,h\left[\alpha_1 h_1\right]\right) \tag{25}$$

The pressure gradient obtained from Eq. (25) can be expressed as:

$$\frac{dp}{dx}=-\left(M^2+\frac{1}{Da}\right)\left(a_3\right) \tag{26}$$

where

$$a_3 = \left(\frac{q-(d_6)(a_1)-(d_7)(a_2)}{d_6(a_1)+d_7(a_2)+(h_2-h_1)} \right),$$

$$d_6 = \left(\frac{\left(\mathrm{Cosh}[\alpha_1 h_2]-\mathrm{Cosh}[\alpha_1 h_1]\right)}{\alpha} \right),$$

$$d_7 = \left(\frac{\left(\mathrm{Sinh}[\alpha_1 h_2]-\mathrm{Sinh}[\alpha_1 h_1]\right)}{\alpha} \right).$$

In the laboratory frame, the flux $Q(x,t)$ is:

$$Q = \int_{h_2}^{h_1} (u+1)\,dy = q-h \tag{27}$$

The average volume flow rate of a peristaltic wave throughout one wave interval is expressed as:

$$\overline{Q} = \frac{1}{T}\int_0^T Q\,dt = q+1+d \tag{28}$$

The pressure gradient can be calculated using Eqs. (26) and (28) as follows:

$$\frac{dp}{dx} = -\left(M^2 + \frac{1}{Da} \right) \times \left(\frac{\left(\overline{Q}-1-d\right)-(d_6)(a_1)-(d_7)(a_2)}{d_6(a_1)+d_7(a_2)+(h_2-h_1)} \right) \tag{29}$$

4. Results and discussion

The goal of the research was to look at the Ohmic heating, Radiation, and Gravity Field in a tapered channel with peristalsis on an MHD Jeffery fluid model. For computations of this study, the following default parameter values are used: ε = 0.2, k_1= 0.1, x = 0.6,t = 0.4, $\theta = \pi/3$, $\phi = \pi/4$, $\lambda_1 = 0.5$, Da = 0.5, $\eta = 1$, M = 1, p = 0.5, $\overline{Q} = 0.2$, d = 2, Br = 0.1, Pr = 2, N = 0.3, $\beta = 0.1$. Unless otherwise specified on the appropriate graph, all graphs relate to these values.

4.1. Validation of the model

We compared the computed numerical findings (Table 1) with the results of Ravi Rajesh and Rajasekhara Gowd [25] in this part. As Ravi Rajesh and Rajasekhara Gowd's method is completely analytical, it serves as a baseline in this comparison. As shown in Table 2, the estimated velocity is compared to the matching velocity distribution values derived by Rajesh and Rajasekhara Gowd's [25] solution. The computed findings for the porosity parameter Da = 0.1, 0.5, 1 are in close agreement with Rajesh and Rajasekhara Gowd's [25] comparable result, indicating that the solution computed is correct and the analysis provided is valid.

4.2. Velocity profile

Fig. 2 demonstrates the variation of the axial velocity (u) with Gravity field (η). It is ascertained from this graph that the velocity of the fluid enhances with increase in η. The fluid of the velocity improved when the Jeffery fluid parameter increased, as illustrated in Fig. 3. We perceive from Fig. 4 that the velocity enhances with increase in M. Fig. 5 presents the impact of Da on u; notice that u increases as Da rises.

Table 1. Velocity distribution for various values of Da.

y value	Da = 0.1	Da = 0.5	D a = 1
-1.25	-1	-1	-1
-0.75	0.1002	0.2894	0.3899
-0.25	0.2975	0.7550	0.9510
0.25	0.2990	0.7598	0.9571
0.75	0.1102	0.308	0.4117
1.25	-1	-1	-1

Table 2. Velocity distribution for various values of Da.

y value	Da = 0.1	Da = 0.5	Da = 1
-1.25	-1	-1	-1
-0.75	0.1043	0.2909	0.3909
-0.25	0.3012	0.7591	0.9540
0.25	0.3041	0.7602	0.9601
0.75	0.1163	0.3102	0.4140
1.25	-1	-1	-1

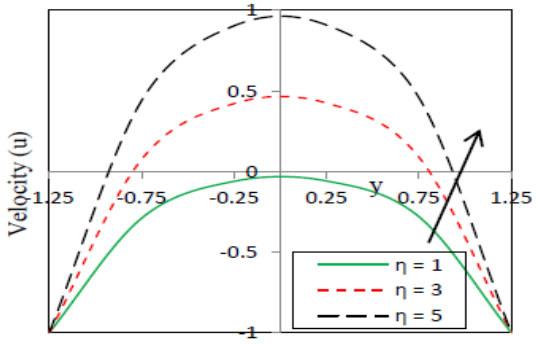

Fig. 2. Impact of η on axial velocity.

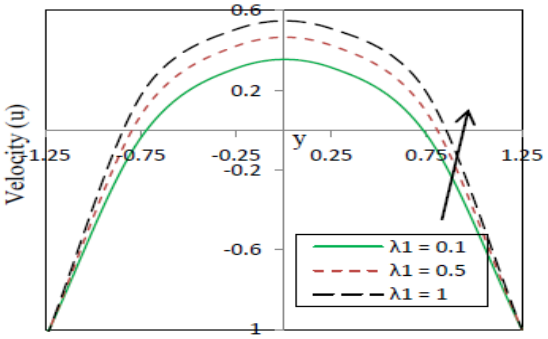

Fig. 3. Impact of λ_1 on axial velocity.

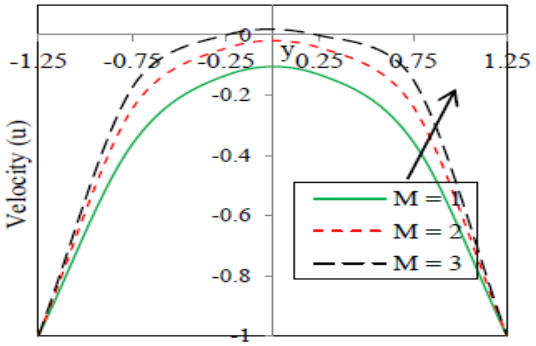

Fig. 4. Axial velocity with M.

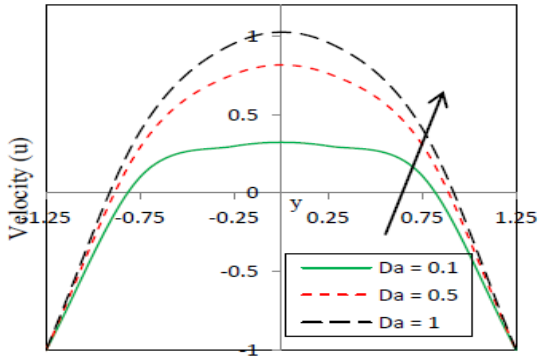

Fig. 5. Axial velocity with Da.

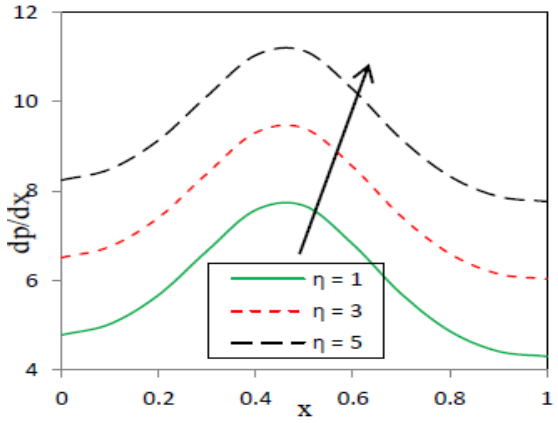

Fig. 6. dp/dx with η.

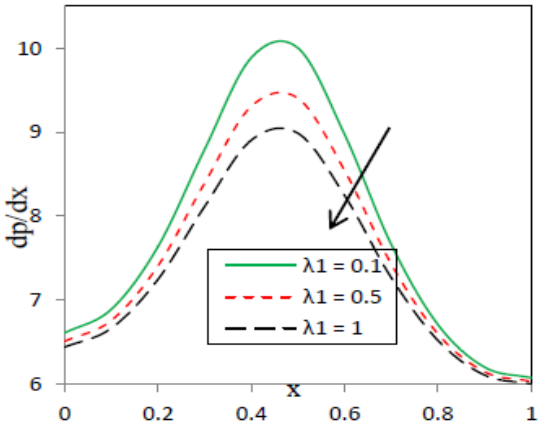

Fig. 7. dp/dx with λ_1.

4.3. Pumping characteristics

4.3.1. Pressure gradient

The aim of Fig. 6 was to study the impact of gravity filed on pressure gradient. We can see in this graph that the pressure gradient of the fluid enhances with an increase in a gravity field. An impact of λ_1 on pressure gradient is portrayed in Fig. 7. The pressure gradient decreases as λ_1 increases, as shown in Fig. 7. Fig. 8 presents the impact of Hartmann number on dp/dx. It is ascertained from this graph that the dp/dx increases when thre is a rise in M. Fig. 9 is drawn to review the impact of the porous parameter on the pressure gradient. We can see from this graph that when the porosity parameter increases, the pressure gradient decreases.

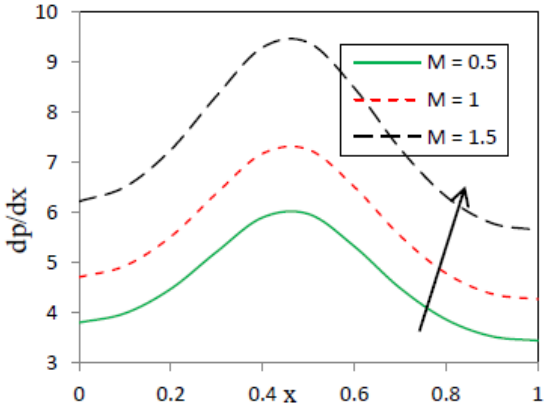

Fig. 8. dp/dx with M.

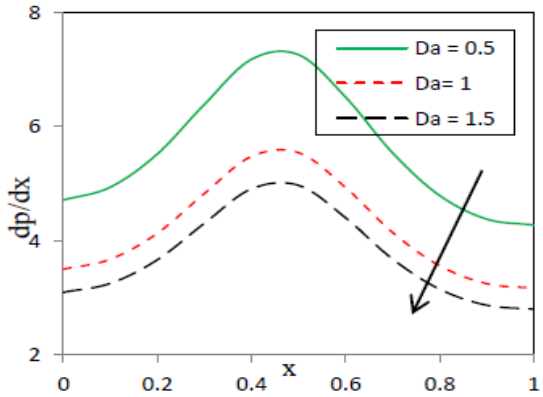

Fig. 9. dp/dx with Da.

4.3.2. Temperature

Fig. 10 depicts the effect of η on the temperature of the fluid. As can be seen in this diagram, when η increases, the temperature of the fluid rises. It can be seen in Fig. 11 that when the Jeffery fluid parameter increases, the fluid temperature drops. As Pr rises, the temperature rises, as can be seen in Fig. 12. Temperature enhances as N increases, as shown in Fig. 13. The aim of Fig. 14 was to study the impact of β on θ. We observe that θ increases as there is an increase in β. From Fig. 15, we notice that as Br rises, the temperature of the fluid increased.

4.3.3. Heat transfer coefficient

Fig. 16 represents the variation in heat transfer coefficient (Z at y = h_1) with Prandtl fluid parameter . It is ascertained from this graph that in region $x \in [0, 0.55]$, the heat transfer coefficient rate diminished whereas in region $x \in [0.55, 1]$, the heat transfer coefficient rises as the Prandtl parameter rises. The impact of N on Z is portrayed in Fig. 17. The heat transfer coefficient in region $x \in [0{,}55\ 1]$ increases as N increases.

Fig. 18 shows that as β increases, the heat transfer coefficient increases in $x \in [0{,}55\ 1]$. Fig. 19 explains the results of Z with λ_1, observe that as λ_1 rises, Z increases in $x \in [0{,}55\ 1]$.

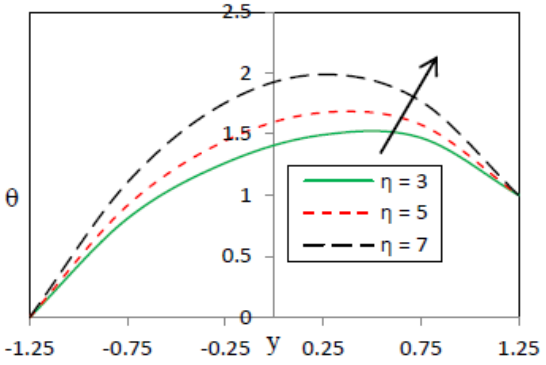

Fig. 10. Temperature with η.

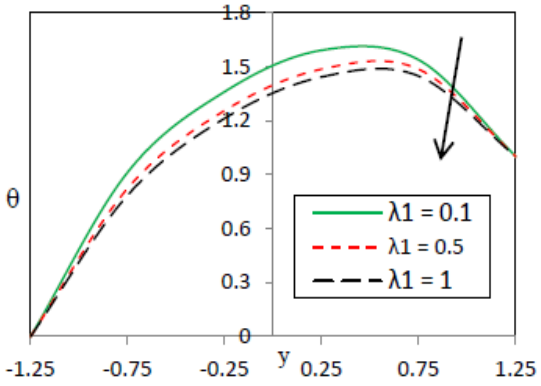

Fig. 11. Temperature with λ_1.

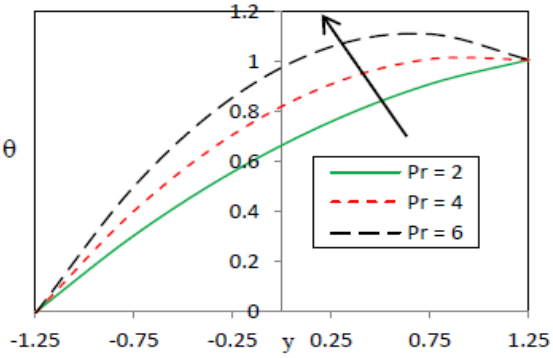

Fig. 12. Temperature with Pr.

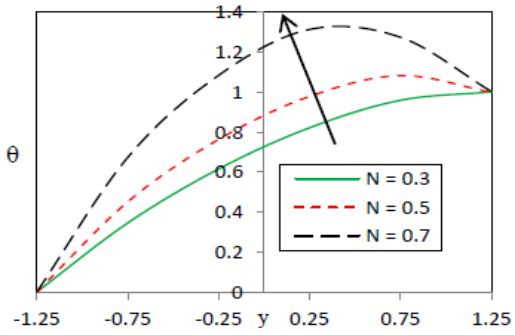

Fig. 13. Temperature with N.

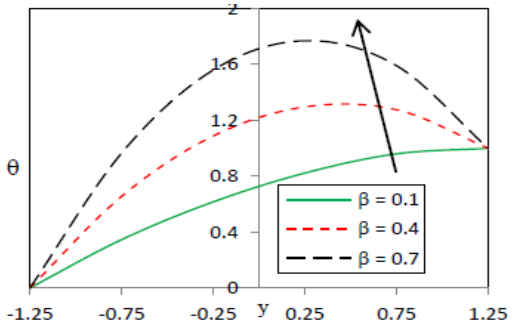

Fig. 14. Temperature with β.

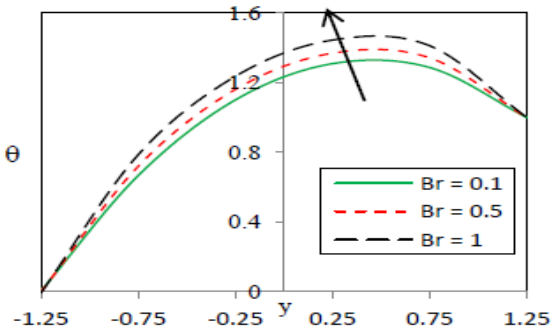

Fig. 15 . Temperature with Br.

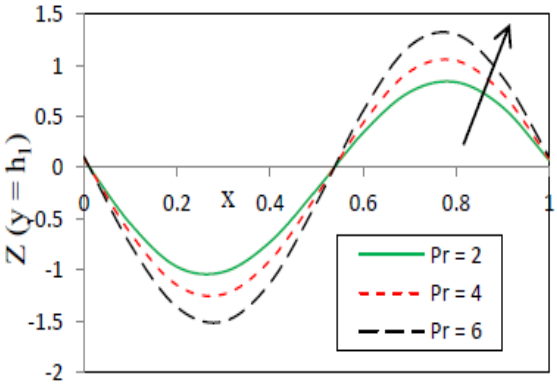

Fig. 16. Heat transfer coefficient with Pr.

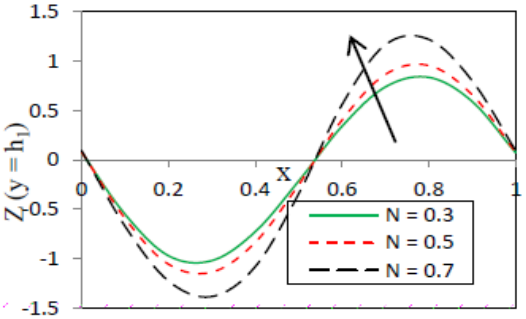

Fig. 17. Heat transfer coefficient with N.

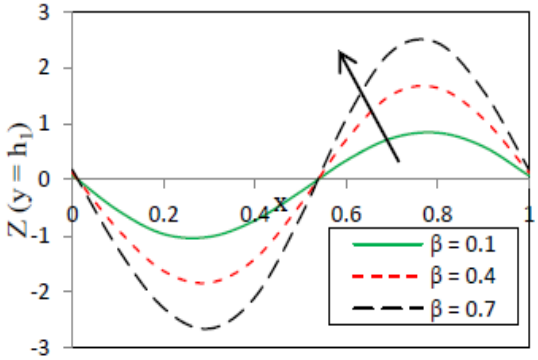

Fig. 18. Heat transfer coefficient with β.

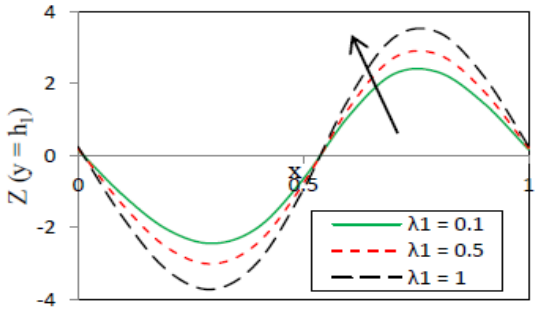

Fig. 19. Heat transfer coefficient with λ_1.

5. Conclusions

The role of Ohmic heating (Joule heating) and Radiation and Gravity Field on MHD Jeffery fluid model in a vertical channel with peristalsis has been investigated. The main outcomes are cited below:

- With an increase in $\eta, \lambda_1, M \text{ and } Da$, the velocity of the fluid increases.
- Increases in η and M increase the pressure gradient, while increases in λ_1 and Da decrease it.

- The temperature of the fluid rises with increases in η, $\Pr$, N, β and Br, but falls with an increase in λ_1
- The rate of heat transfer coefficient enhances in $x \in [0.55,1]$ with a rise in $\Pr, N, \beta$ *and* λ_1.

References

[1] M. Y. Jaffrin and A. H. Shapiro, "Peristaltic pumping", *Annu. Rev. Fluid Mech.*, Vol. 3, No. 3, pp. 13-37, (1971).

[2] Y. C. Fun and C. S. Yih, "Peristaltic transport", *J. Appl. Mech*., Vol. 35, No. 4, pp. 669-675, (1968).

[3] A. H. Shapiro, M. Y. Jaffrin and S.L. Weinberg, "Peristaltic pumping with long wavelengths at low Reynolds number", *J. Fluid Mech.*, Vol. 37, No. 4, pp. 799-825, (1969).

[4] M. Kothandapani and J. Prakash, "Influence of thermal radiation and magnetic field on peristaltic transport of a Newtonian nanofluid in a tapered asymmetric porous channel", *J. Nanofluids*, Vol. 5, No. 3, pp. 363-374, (2016).

[5] M. M. Bhatti, A. Zeeshan, R. Ellahi and G. C. Shit, "Mathematical modeling of heat and mass transfer effects on MHD peristaltic propulsion of two-phase flow through a Darcy-Brinkman-Forchheimer porous medium", *Adv. Powder Technol.*, Vol. 29, No. 5, pp. 1189-1197, (2018).

[6] S. K. Ghosh, O. Anwar Beg and J. Zueco, "Hydromagnetic free convection flow with induced magnetic field effects", *Meccanica*, Vol. 45, No. 2, pp. 175-185, (2010).

[7] N. Ameer Ahamad, S. Ravikumar, and Kalimuthu Govindaraju, "Influence of radiation on MHD peristaltic blood flow through a tapered channel in presence of slip and joule heating", *AIP Conf Proc.*, Vol.1863, No. 1, pp. 560091, (2017).

[8] O. D. Makinde, Z. H. Khan, W. A. Khan and M. S. T Shehla, "Magneto-Hemodynamics of Nanofluid with heat and mass transfer in a slowly varying symmetrical channel", *Int. J. Eng. Res. Africa.*, Vol. 28, No. 1, pp. 118-141, (2017).

[9] A. Sinha and J. C. Misra, "Numerical study of flow and heat transfer during oscillatory blood flow in diseased arteries in presence of magnetic fields", *Appl. Math. Mech. - Engl. Ed.*, Vol. 33, No. 5, pp. 649-662, (2012).

[10] S. Akram and S. Nadeem, "Significance of Nanofluid and partial slip on the peristaltic transport of a non-Newtonian fluid with different wave forms", *IEEE Tran. Nanotech.*, Vol. 13, No. 2, pp. 375-385, (2014).

[11] R. Ellahi, "The effects of MHD and temperature dependent viscosity on the flow of non- Newtonian nanofluid in a pipe- Analytical solutions", *Appl. Math. Modl.*, Vol. 37, No. 3, pp. 1451-1467, (2013).

[12] M. M. Rashidi, M. Nasiri, M. Khezerloo and N. Laraqi, "Numerical investigation of magnetic field effect on mixed convection heat transfer of nanofluid in a channel with sinusoidal walls", *J. Magn. Magn. Mater.*, Vol. 401, No. 3, pp. 159-168, (2016).

[13] M. Gnaneswara Reddy and O. D. Makinde "MHD peristaltic transport of Jeffrey nanofluid in an asymmetric channel", *J. Mol. Liq.*, Vol. 223, No.11, pp. 1242-1248, (2016).

[14] M. M. Bhatti, R. Ellahi and A. Zeeshan, "Study of variable magnetic field on the peristaltic flow of Jeffrey fluid in a non-uniform rectangular duct having compliant walls", *J. Mol. Liq*., Vol. 222, No. 10, pp. 101-108, (2016).

[15] T. Hayat, H. Zahir, A. Tanveer and A. Alsaedi, "Soret and Dufour effects on MHD peristaltic transport of Jeffrey fluid in a curved channel with convective boundary conditions", *PLoS ONE*, Vol. 12, No. 2, e0164854, (2017).

[16] M. Gnaneswara Reddy, K. Venugopal Reddy and O. D. Makinde, "Heat transfer on MHD peristaltic rotating flow of a Jeffrey fluid in an asymmetric channel", *Int. J. Appl. Comput. Math*., Vol. 3, No. 4, pp. 3201-3227, (2017).

[17] C. Veeresh, S. V. K. Varma, A. G. Vijaya Kumar, M. Umamaheswar and M. C. Raju, "Joule heating and thermal diffusion effects on MHD radiative and convective casson fluid flow past an oscillating semi-infinite vertical porous plate", *FHMT*, Vol. 8, No. 1, pp. 1-8, (2017).

[18] K. Vajravelu, S. Sreenadh and P. Lakshminarayana, "The Influence of heat transfer on peristaltic transport of a Jeffrey fluid in a vertical porous stratum", *Commun. Nonlinear Sci. Numer. Simul.*, Vol. 16, No. 8, pp. 3107-3125, (2011).

[19] N. T. M. Eldabe, M. O. Shaker and S. A. Maha, "Peristaltic flow of MHD Jeffrey fluid through porous medium in a vertical channel with heat and mass transfer with radiation", *J. Nanofluids*, Vol. 7, No. 3, pp. 595-602, (2018).

[20] S. K. Asha and G. Sunitha, "Effect of joule heating and MHD on peristaltic blood flow of Eyring–Powell nanofluid in a non-uniform channel", *J. Taibah Univ. Sci.*, Vol. 13, No. 1, pp. 155-168, (2019).

[21] N. Ali Sha, N. Ahmed, T. Elnaqeeb and M. Mehdi Rashidi, "Magnetohydrodynamic free convection flows with thermal memory over a moving vertical plate in porous medium", *J. Appl. Comput. Mech.*, Vol. 5, No. 1, pp. 150-161, (2019).

[22] A. J. Chamkha, A. S. Dogonchi and D. D. Ganji, "Magneto-hydrodynamic flow and heat transfer of a hybrid nanofluid in a rotating system among two surfaces in the presence of thermal radiation and Joule heating", AIP Adv., Vol. 9, No. 2, pp. 025103-1 - 025103-14, (2019).

[23] M. Kothandapani, J. Prakash and V. Pushparaj, "Analysis of heat and mass transfer on MHD peristaltic flow through a tapered asymmetric channel", *J. Fluids*, Vol. 2015, No. 12, pp. 1-9, (2015).

[24] A. C. Cogley, S. E. Giles and W. G. Vincenti, "Differential approximation for radiative transfer in nongrey gas near equilibrium", *AIAA J.*, Vol. 6, No. 3, pp. 551-553, (1968).

[25] R. Rajesh and Y. Rajasekhara Gowd, "Impact of Hall Current, Joule Heating and Mass Transfer on MHD Peristaltic Hemodynamic Jeffery Fluid with Porous Medium under the Influence of Chemical Reaction", *Chem. Eng. Trans.*, Vol. 71, No. 9, pp. 997-1002, (2018).

How to cite this paper:

S. Ravikumar, D. Vijaya Sekhar and SK. Abzal, " Role of ohmic heating and radiation on magnetohydrodynamic Jeffery fluid model,", *J. Comput. Appl. Res. Mech. Eng.*, Vol. 11, No. 2, pp. 317-327, (2022).

DOI: 10.22061/JCARME.2021.4994.1607

URL: https://jcarme.sru.ac.ir/?_action=showPDF&article=1595